Carbohydrate Polymers 89 (2012) 213–221

Contents lists available at SciVerse ScienceDirect

Carbohydrate Polymers

journal homepage: www.elsevier.com/locate/carbpol

Analysis of crystallinity changes in cellulose II polymers using carbohydrate-binding modules

Ján Široký[a,c], Thomas A.S. Benians[b], Stephen J. Russell[a], Thomas Bechtold[c], J. Paul Knox[b], Richard S. Blackburn[a,*]

[a] Sustainable Materials Research Group, Centre for Technical Textiles, University of Leeds, Leeds LS2 9JT, UK
[b] Centre for Plant Sciences, Faculty of Biological Sciences, University of Leeds, Leeds LS2 9JT, UK
[c] Christian Doppler Laboratory for Textile and Fiber Chemistry in Cellulosics, Research Institute of Textile Chemistry and Textile Physics, University of Innsbruck, Höchsterstraße 73, A-6850 Dornbirn, Austria

ARTICLE INFO

Article history:
Received 24 January 2012
Received in revised form 27 February 2012
Accepted 29 February 2012
Available online 7 March 2012

Keywords:
Cellulose II
Lyocell
Fiber
Crystallinity
Amorphous
ATR FT-IR spectroscopy
Sodium hydroxide
Carbohydrate-binding module
Fluorescence microscopy

ABSTRACT

Carbohydrate-binding modules (CBMs) are a set of tools that can be used as molecular probes for studying plant cell walls and cellulose-based substrates. CBMs from enzymes of bacterial and fungal origin present a range of recognition capabilities for crystalline and amorphous cellulose. Here cellulose-directed CBMs have been used to visualize and quantify crystallinity changes in cellulose II-based polymers following NaOH treatment. Cellulose II polymers used were in the form of lyocell fibers, which are derived from eucalyptus wood pulp. The supramolecular structure, morphology, and existence of 'skin-core' model in the fiber were examined using CBM-labeling techniques. Changes in cellulose crystallinity showed maxima at 3.33 mol dm^{-3} NaOH (under treatment conditions of 49 N m^{-1} at 25 °C) and 4.48 mol dm^{-3} NaOH (under treatment conditions of 147 N m^{-1} at 40 °C); CBM methods were also suitable for quantifying changes within amorphous regions. Quantification of crystallinity changes using CBM labeling techniques was achieved in combination with image analysis, which was shown to reflect the same crystallinity changes as measured using ATR-FTIR methods. It was demonstrated that CBM-labeling techniques were able to validate the proposed 'skin-core' model of lyocell fibers, comprising a semi-permeable fiber skin and a porous core.

1. Introduction

Carbohydrate-binding modules (CBMs) are found in many carbohydrate-active enzymes. CBMs are non-catalytic protein modules that promote the association of the enzyme with the substrate and their main function is to increase the catalytic efficiency of the enzyme against soluble and/or insoluble substrates. In the Carbohydrate-Active enZYmes (CAZY) Database, a CBM is defined as a contiguous amino acid sequence within a carbohydrate-active enzyme with a discrete fold having carbohydrate-binding activity (Hashimoto, 2006; McCartney et al., 2006). CBMs with the capacity to bind cellulose are associated with enzymes that hydrolyze both cellulose and other cell wall polymers such as xylan, mannan, pectin, and non-cellulosic-glucans (Hogg et al., 2003; Kellett et al., 1990; McKie et al., 2001). CBMs are grouped into sequence-based families and are named after the family in which they are located (*e.g.* a family 4 CBM is designated CBM4). CBMs from families 1, 2a, 3a, 5, and 10 are classified as type A CBMs, which bind to crystalline polysaccharides, predominantly cellulose (Jamal, Nurizzo, Boraston, & Davies, 2004), as the topography of the ligand recognition site is conserved presenting a flat surface comprising predominantly aromatic residues, which interact with the multiple planar cellulose chains found in crystalline cellulose (Raghothama et al., 2000; Xu et al., 1995). Type B CBMs do not bind to the planar surface of crystalline polysaccharides but recognize isolated saccharide chains. Three well characterized examples of cellulose-binding type B CBMs are found in families 4, 17, and 28. The ligand-binding sites in these protein modules comprise extended clefts or grooves that accommodate individual glycan chains in non-crystalline regions of cellulose (Boraston, Nurizzo, et al., 2011; Jamal et al., 2004); they display similar cellulose binding properties, although competition studies indicate that these modules recognize different substructures within amorphous cellulose (Araki, Karita, Tsuchiya, Kondo, & Goto, 2010; McLean et al., 2002).

Indirect immunofluorescence labeling using recombinant CBMs is commonly used to provide a visual representation of the cellulose plant structure, particularly the variation in cell wall or other cellulose I substrates like wood tissues and Valonia cellulose recognition of both crystalline and amorphous regions (Boraston, Kwan,

* Corresponding author. Tel.: +44 113 343 3757; fax: +44 113 343 3704.
E-mail address: r.s.blackburn@leeds.ac.uk (R.S. Blackburn).

0144-8617/$ – see front matter © 2012 Elsevier Ltd. All rights reserved.
doi:10.1016/j.carbpol.2012.02.073

Chiu, Warren, & Kilburn, 2003; Dagel et al., 2011; Jamal et al., 2004; Kawakubo et al., 2010; Lehtio et al., 2003). The most effective binders to visualize cellulose and other plant cell walls are CBM3a and CBM28 due to their known affinities to crystalline and amorphous cellulose respectively (Jamal et al., 2004; McCartney et al., 2006). On the basis of previous research (Blake et al., 2006; McCartney et al., 2006; McCartney, Gilbert, Bolam, Boraston, & Knox, 2004), this method has been employed first time as a tool for quantitative and microscopic analysis of changes in cellulose II-based polymers on the supramolecular level, and to monitor its changes, for example, caused by NaOH treatment.

The recognition of cellulose in the context of cell walls by diverse families and types of CBM has not been systematically examined. It has been previously demonstrated that CBMs directly coupled to fluorophores or with His tag appendages can be used to investigate the localization of these proteins when bound to target polymers in the context of cell wall composites (Blake et al., 2006; McCartney et al., 2006, 2004), wood tissues (Kawakubo et al., 2010) or Valonia cellulose crystallites (Dagel et al., 2011). Herein, alkali-treated lyocell fibers, a cellulose II-based polymer, were examined. Lyocell fibers are derived from eucalyptus wood pulp and consist of a linear 1,4-β-glucan polymer where the units are able to form highly ordered structures (crystalline cellulose II), as a result of extensive interaction through intra- and intermolecular hydrogen bonding of the three hydroxyl groups in each cellulose unit as well as low ordered structures (amorphous cellulose). Lyocell has a high degree of crystallinity (up to 70–80%) which is a consequence of higher orientation during stretching and formation of fibers; lyocell fibers have the thinnest and longest crystallites, even the amorphous regions are oriented along the fiber axis (Crawshaw & Cameron, 2000). Lyocell fibers have a microfibrillar structure because a portion of the molecular chains aggregate to form microcrystals while recrystallizing along the chains, whereas the remaining chains exist in the amorphous phase as links between these two phases (Okano & Sarko, 1984). In the crystalline regions of cellulose II polymers, the layered structure is very regular, so the length of hydrogen bonds between molecules is the same (Kolpak & Blackwell, 1976; Kono & Numata, 2004; Langan, Nishiyama, & Chanzy, 1999). Current knowledge assumes the structure of cellulose II is an anti-parallel arrangement of cellulose chains with some inter-sheet hydrogen bonding, generally leading to a perfectly distributed symmetrical structure, and a C(6) conformation of CH_2OH group is of *gauche-trans* conformation (gt) as well as a mixed conformation of *gauche-trans* and *trans-gauche* (tg) may be observed at significance level of better than 5% resulted from X-ray refinement (Klemm, Philipp, Heinze, Heinze, & Wagenknecht, 1998). Although, the different assessments are available like that based on molecular dynamics (MD) simulations done by Kroon-Batenburg, Bouma, and Kroon (1996). Therein, the authors propose the structure of regenerated cellulose fibers as an anti-parallel mixed conformation of gt and gt, which has slightly higher the average relative potential energy than that of a mixed gt and tg conformation. They also suggested that favorable arrangements of mercerized structure is a parallel mixed conformation of gt and gt. Alkali treatment has a substantial influence on morphological, molecular and supramolecular properties of cellulose, causing changes in crystallinity, pore structure, accessibility, stiffness, unit cell structure and orientation of fibrils in cellulosic fibers (Široký et al., 2008). Treatment with alkali can improve mechanical and chemical properties of cellulose fibers such as dimensional stability, fibrillation tendency, tensile strength, dyeability, reactivity, luster and fabric smoothness. Factors such as the concentration of NaOH, treatment temperature, applied tension, residence time, source of cellulose, physical state of cellulose (fibril, fiber, yarn or fabric), and degree of polymerization have an effect on the properties and degree of change upon treatment (Heinze & Wagenknecht, 1998; Široký, Blackburn, Bechtold, Taylor, & White, 2010).

Previous research has described how studies of crystallinity and morphology of cellulose have progressed, and how changes in cellulose II crystallinity and morphology due to sodium hydroxide treatment may be analyzed using techniques such as ATR-FTIR (Široký et al., 2010) or dye sorption (Široký, Blackburn, Bechtold, Taylor, & White, 2011). Recently within our research group a similar investigation has been achieved for cellulose I (two species of cotton) using a similar attempt to quantify obtained fluorescence micrographs of bound CBM2a, CBM3a, CBM4-1, and CBM17 (Kljun et al., 2011); it was demonstrated that the CBMs used displayed a greater ability to detect early crystallinity changes in cotton subject to treatment with 0–8 mol dm^{-3} sodium hydroxide, in comparison with analysis by XRD and ATR-FTIR.

The work herein describes the use of immunoassay labeling techniques using CBMs in combination with fluorescence microscopy to monitor changes to the crystallinity of cellulose II polymers when treated with increasing concentrations of aqueous sodium hydroxide solution (0.00–7.15 mol dm^{-3}) under varied temperature (25 or 40 °C) and tension (49 or 147 N m^{-1}); crystallinity changes are quantified in combination with image analysis methods. The results of bound CBMs are compared with crystallinity changes monitored using Attenuated Total Reflectance Fourier-Transform Infrared (ATR-FTIR) spectroscopy.

2. Experimental

2.1. Materials

Plain-woven (1/1 weave), desized, scoured lyocell fabrics (Tencel, 140 g m^{-2}, comprised of 50/1 Nm yarn) used for this observation were kindly supplied by Lenzing AG, Austria. Technical grade NaOH (*ca.* 50%, w/w) was used in formulating the alkali solutions used in treatments, with *Lyogen MC* (Clariant, Basel, Switzerland) added as wetting agent. Analytical grade acetic acid was used in formulating the neutralization liquor.

CBMs types used in this research are shown in Table 1; all CBMs were of the fold 1 (β-sandwich) family (Hashimoto, 2006; Jamal et al., 2004; McCartney et al., 2004). All CBMs were kindly supplied by Prof. Harry Gilbert, Department of Biological and Nutritional Sciences, Newcastle University; 3D structures of the CBMs are shown in Blake et al. (2006). All other chemicals were supplied by Sigma–Aldrich.

Table 1
Cellulose-directed CBMs used in this study.

CBM probe	Fold family	Fold	Type	Epitope	Reference
CBM2a	1	β-Sandwich	A	Crystalline cellulose	Bolam et al. (1998)
CBM3a	1	β-Sandwich	A	Crystalline cellulose	Tormo et al. (1996)
CBM10	5	OB fold	A	Crystalline cellulose	Jamal et al. (2004), Hashimoto (2006)
CBM4-1	1	β-Sandwich	B	Amorphous cellulose	Tomme, Creagh, Kilburn, and Haynes (1996)
CBM17	1	β-Sandwich	B	Amorphous cellulose	Boraston, Chiu, Warren, and Kilburn (2000)
CBM28	1	β-Sandwich	B	Amorphous cellulose	Jamal et al. (2004), Hashimoto (2006)

OB = oligonucleotide/oligosaccharide bindings.

2.2. Sodium hydroxide treatment

The continuous process of alkali treatment of lyocell was done with a specially designed washer, unique semi-scale equipment simulating a real industrial process. The equipment is divided into four stages: treatment, stabilization, washing, and neutralization. In the treatment stage, NaOH concentration, applied tension and temperature varied. Due to changes in the concentration in the treatment stage (caused by process), the "effective" concentration of alkali was established at 0.0, 2.53, 3.33, 4.48, 4.65 and 7.15 mol dm^{-3} for treatment bath and 0.0, 0.73, 1.08, 1.18, 1.48 and 2.15 mol dm^{-3} for stabilization bath (initially set up at 20% of treatment NaOH concentration), which is described in detail in our previous work (Široký et al., 2009). Washing was performed in water alone at 80 °C; neutralization was carried out using 2 g dm^{-3} acetic acid (80%, v/v) at 80 °C. After the treatment process, samples were dried continuously in a stenter at 130 °C, but not as part of the continuous treatment.

Tension in treatment compartment was applied at 49 or 147 N m^{-1}, stabilization compartment of 147 N m^{-1} tension, and tension in washing and neutralization compartments was applied at 49 N m^{-1}. During the alkali treatment stage the temperature of the solution was set at 25 °C or 40 °C, and in the stabilization stage the temperature was 60 °C. In each compartment, the volume of the liquor was 20 dm^3. The speed of passage of fabric through the system was set at 2 m min^{-1}. Further details about the all conditions and adjustments of continuous alkali pre-treatments are available in our previous work (Široký et al., 2009).

2.3. Attenuated total reflectance Fourier transform infrared (ATR-FTIR)

Samples were subjected to ATR-FTIR spectroscopy (at four different points in the sample) using a Perkin-Elmer Spectrum BX spotlight spectrophotometer with diamond ATR attachment. Scanning was conducted from 4000 to 600 cm^{-1} with 64 repetitious scans averaged for each spectrum. Resolution was 4 cm^{-1} and interval scanning was 2 cm^{-1}. Prior to measurement, samples were conditioned in a standard atmosphere of 65 ± 2% relative humidity and 20 ± 2 °C for 48 h, then and held in a desiccator over P_2O_5 to maintain the same atmosphere as the FTIR measurement equipment was not located in the same place. Obtained spectra were normalized to the absorbance of the O–H in-plain deformation band at 1336 cm^{-1} due to any obtained changes in this band among all examined samples. Total crystallinity index (TCI) was obtained from the ratio of the intensity of the absorbance bands at 1372 cm^{-1} and 2892 cm^{-1} ($\alpha_{1372/2892}$), lateral order index (LOI) was obtained from the ratio of the intensity of the absorbance bands at 1418 cm^{-1} and 894 cm^{-1} ($\alpha_{1418/894}$), and hydrogen bond intensity (HBI) was obtained from the ratio of the intensity of the absorbance bands at 3336 cm^{-1} and 1336 cm^{-1} ($\alpha_{3336/1336}$). Further details of these absorbance bands, the respective crystallinity indices and their calculation are described in Široký et al. (2010).

2.4. Low temperature LR resin embedding for sectioning

An acrylic embedding resin system (LR resin) was used for sectioning of immunofluorescently labeled lyocell fibers which

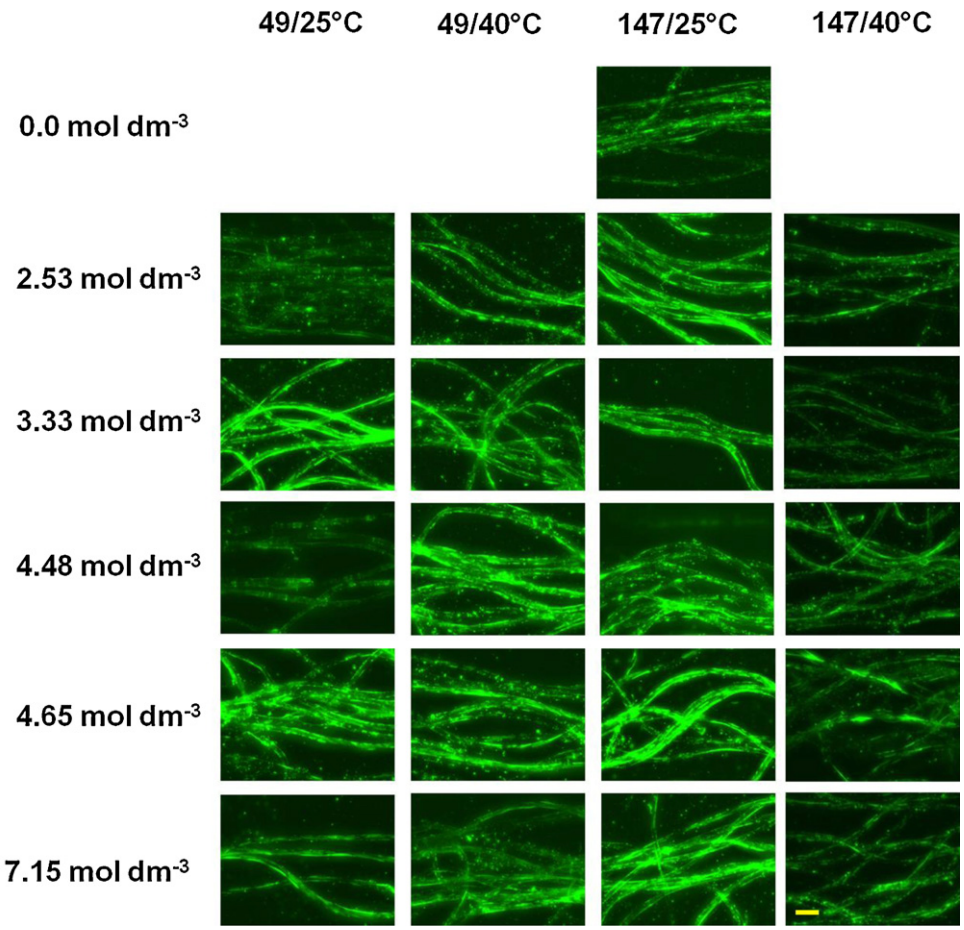

Fig. 1. Indirect immunofluorescence detection of bound CBM3a after NaOH and pectate lyase treatments of Lyocell. Scale for all pictures is 10 μm.

enables excellent preservation of wide variety of biological (Bendayan, Nanci, & Kan, 1987; Newman & Hobot, 1987; Timms, 1986; Wells, 1985) and plant (Craig & Miller, 1984; Hess, 2003; Lonsdale, McDonald, & Jones, 1999) tissues. The embedding is one-step single component resin system of ultra low viscosity close to that of water. Formaldehyde fixed lyocell fibers were dehydrated with graded ethanol series (10%, 20%, 30%, 50%, 70%, 90%, 100%, and 100%) at −20 °C for 10 min with each concentration. Hard LR white resin was infiltrated three times at room temperature for 60 min each time, with the final infiltration left overnight in polymerization capsules. Polymerization of the resin embedded fiber was completed at 65 °C for 24 h. Sections were cut using glass knives, and cut to a thickness of 0.5 μm and placed on *Vectabond*-coated multi-well microscope slides.

2.5. In situ fluorescence imaging of CBM recognition of lyocell fibers

Samples were incubated in 5% milk powder/phosphate buffer solution (PBS) for 30 min and then rinsed off once with PBS. Primary CBMs were added at 1 in 50 dilution and were incubated for at least 90 min at room temperature with shaking. After that, samples were washed three times with 5% PBS, 5 min per wash. Secondary antibody (anti-his, mouse) was added, diluted 1 in 1000 in 5% milk powder/PBS and incubated for at least 90 min. Samples were washed again three times with 5% PBS, 5 min per wash. Tertiary antibody (FITC-anti mouse) was added, diluted 1 in 50 in 5% milk powder/PBS and incubated for at least 90 min. Samples were washed three times with 5% PBS, 5 min per wash. Samples were kept in the dark, to stop the FITC fluorochrome from degrading. At the last stage, Citifluor was added in PBS/glycerol to the slide to prevent fluorescence fading. After adding the coverslip, slides were kept in the dark except for viewing.

2.6. Digital image analysis

Immunofluorescence imaging was combined with differential interference contrast imaging using an Olympus BX61 microscope equipped with differential interference contrast optics and epifluorescence irradiation. Images achieved for samples labeled with CBMs showed a green color (for CBM2a, CBM3a and CBM10 this was observed where crystalline cellulose was present, for CBM28, CBM4-1, and CBM17 this was observed where amorphous cellulose was present).

The images were manipulated to allow quantification of the data within the image. Image processing involves manipulating and improving images by the application of mathematical functions, which enables various tasks to be carried out, including image enhancement, image analysis, and image-coding. In recent years, the improvement in computer technology has had a positive effect on textile research, finding application in fiber-cross-section analysis, maturity measurement of cotton, measurement of pore-size distribution, analysis of fiber crimp, and analysis of yarn structure (Behera, 2004).

The image enhancement was performed using Image Pro Plus 6.5 software. Firstly, contrast enhancement was made applying brightness and contrast adjustments; it was kept constant for all evaluated images, to raise the contrast between fluorescent parts

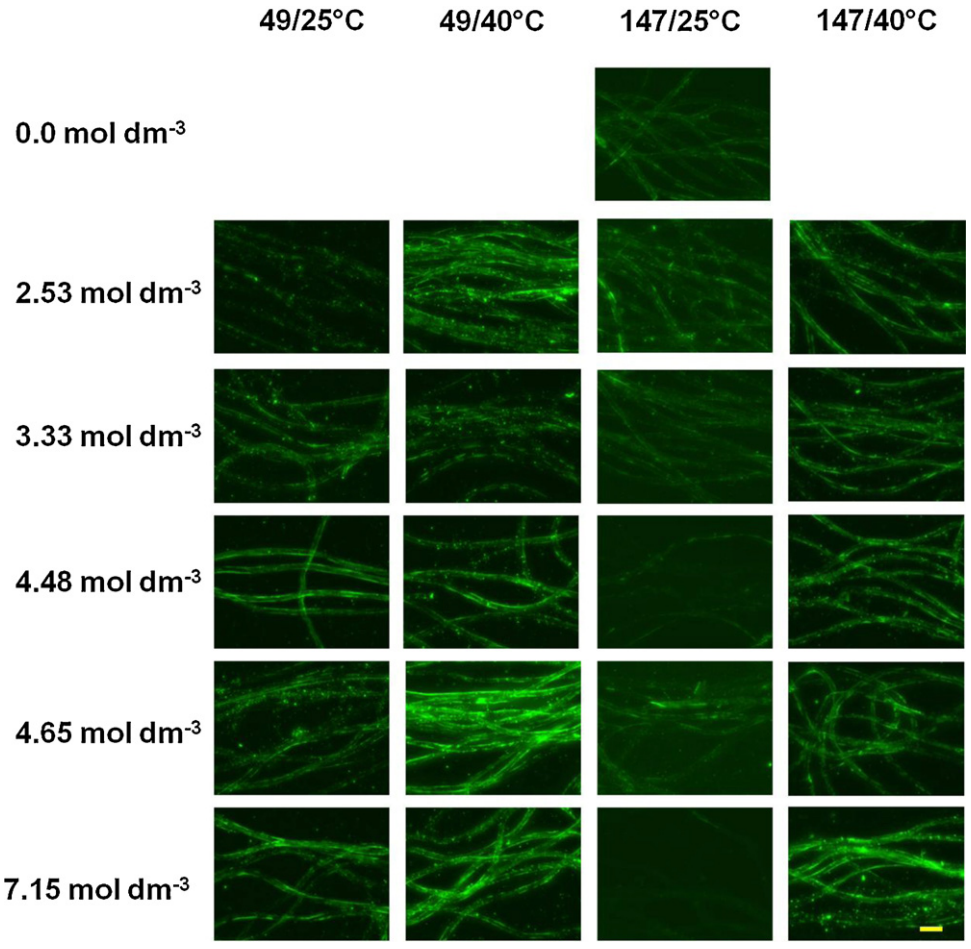

Fig. 2. Indirect immunofluorescence detection of bound CBM28 after NaOH and pectate lyase treatments of Lyocell. Scale for all pictures is 10 μm.

of both crystalline and amorphous regions (green) and dark (black) background. Additionally, Hi Gauss filters were applied for evaluation of crystalline or amorphous regions, which enhances fine image details which introduce less noise. To quantify changes in crystalline and amorphous phases, squares of specific size (112.2 μm × 91.3 μm) were drawn within each picture (total area 291.7 μm × 222.2 μm) in Image Pro Plus 6.5 software. This technique was used to count the dark objects and their sum area within the squares; software statistics were applied based on five repetitions. The obtained results were re-calculated to quantify the bright area, corresponding to % bound immunofluorescent CBMs relative to the total fiber visible in the image.

3. Results and discussion

Recognition of different phases of cellulose and cell walls respectively visualized by cellulose-binding CBMs is a fascinating and also challenging field. Potentially immunoassay labeling could yield more detailed information on where the changes in the fiber occurs, in comparison with most commonly used techniques, *e.g.* FT-IR, X-ray diffraction, SAXS, *etc.*, that only measure and give an idea about the changes within the crystalline phase; none of these methods are able to effectively define changes in amorphous phases. Both CBM3a and CBM28 present a planar hydrophobic face and CBM3a likely binds to the hydrophobic (110) face of cellulose crystal (Valonia cellulose) (Lehtio et al., 2003), experimentally obtained by transmission electron microscopy (TEM), with the three surface aromatic residues (tyrosine) in these proteins stacking against the pyranose rings of the glucose molecules. It appears that this type of CBM possibly makes a few significant hydrogen bonds with the microfibrillar cellulose structure and also, it is possible that the polar side chains in the binding face of this CBM may interact with the matrix polysaccharides that are in intimate contact with the cellulose microfibrils, and these hydrogen bonds may grant the variation in specificity observed (McCartney et al., 2006).

Figs. 1 and 2 show the captured images of CBM3a and CBM28 binding to crystalline and amorphous cellulose, respectively, at various treatment conditions, NaOH concentration of 0.00–7.15 mol dm^{-3}, tension of 49 or 147 N m^{-1} and temperature of 25 °C or 40 °C. Both CBMs bind well with cellulose II-based polymers, but it is noted that CBM3a binds only to crystalline and CBM28 binds only to amorphous regions of cellulose, as indicated in the figures. In general, it is observed that there is a significantly high proportion of crystalline regions within the structure of lyocell fibers; it is well-known that their degree of crystallinity is highest among regenerated cellulosics. Analysis with CBMs shows that treatment tension, treatment temperature, and, primarily, NaOH concentration have a significant influence on changes in both crystalline and amorphous regions. From Fig. 1 (CBM3a), it can be seen that the brightest (light green) parts were detected under the following treatment conditions of 3.33 mol dm^{-3} NaOH, 49 N m^{-1} tension, at 25 °C, and 4.48 mol dm^{-3} NaOH, 147 N m^{-1} tension, at 40 °C. From Fig. 2 (CBM28), a strong fluctuation is obtained, which may indicate a greater sensitivity of amorphous regions to mechanical (applied tension), chemical (NaOH concentration) as well as thermal (treatment temperature) influence in the treatment process of cellulose II-based polymers than their crystalline-binding counterparts.

These findings may reflect those of Boraston et al. (2003), in that the chains of amorphous cellulose, known as shapeless cellulose, could posses two or more different “physical forms” or

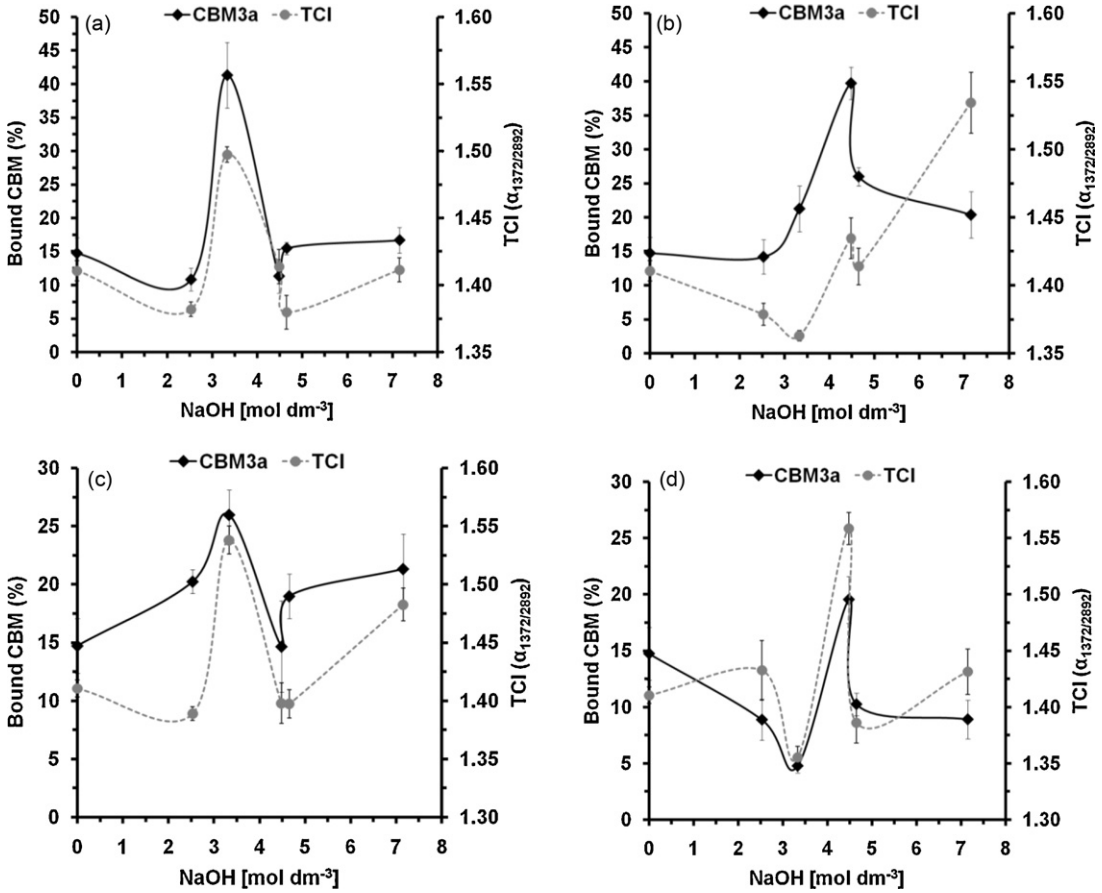

Fig. 3. Comparison of bonded CBM3a with TCI (Široký et al., 2010) with increasing NaOH concentration in treatment stage, under varying tension (49 or 147 N m^{-1}) and temperature (25 or 40 °C) in treatment stage of continuous alkali treatment: (a) 49/25; (b) 49/40; (c) 147/25; (d) 147/40.

"substructures". Therefore, the affinity and/or discrimination of CBM28 may vary with these different amorphous forms. This is certainly worthy of further investigation, but was not an intention herein.

Image Pro Plus 6.5 software was used to quantify the changes in crystalline or amorphous regions, which were obtained from bound CBMs (illustrated in Figs. 1 and 2). These quantified values and comparison of bonded CBMs to crystalline regions of cellulose II-based polymers (as discriminated by CBM3a) were compared with previously obtained total crystallinity index (TCI) and lateral order index (LOI) data (Široký et al., 2010), shown in Figs. 3 and 4, respectively; in general TCI and LOI increase with increase in crystallinity. A detailed explanation of the theory concerning the definition and application of crystallinity indices is provided in our previous work (Široký et al., 2010).

It can be seen that all conditions applied have a substantial effect on re-organization of cellulose on the supramolecular level and/or changes of the crystalline ratio, thus the ratio of amorphous regions varies as well. Two maxima for crystalline CBM bindings were observed, at a concentration of 3.33 mol dm^{-3} NaOH for samples treated at 25 °C, and at 4.48 mol dm^{-3} NaOH for samples treated at 40 °C; similar trends were obtained by ATR-FTIR spectroscopy analysis of crystallinity changes (Široký et al., 2010), which is demonstrated in Figs. 3 and 4. There is little divergence between these two methods; however, the method proposed herein brings the benefit of unique insights and visualization of the supramolecular alterations, respectively, as well as quantification of these alterations. In contrast, ATR-FTIR provides fast qualitative analysis with a minimum sample preparation to assess the crystallinity of porous substrates (Široká, Široký, & Bechtold, 2011) and therefore, it is still of significant importance. Of other methods, X-ray diffraction (XRD) cannot diffract amorphous regions (correction of diffuse scattering from amorphous structure is required) (Barnette et al., 2011; Thygesen, Oddershede, Lilholt, Thomsen, & Stahl, 2005), and results obtained are dependent on the used calculation technique (Thygesen et al., 2005). Cross polarization solid-state ^{13}C NMR is complicated for routine analysis, and simpler NMR analysis, has the problem of overlapping amorphous elements with crystalline ones, which must be deconvoluted from the amorphous spectrum (Park, Baker, Himmel, Parilla, & Johnson, 2010; Park, Johnson, Ishizawa, Parilla, & Davis, 2009).

Crystallinity changes described above may have been attributed by the degree of swelling, which at its maximum (between 3.00 and 3.75 mol dm^{-3}) decreases with increasing temperature of the treatment liquor (Warwicker, 1969). In addition, when the substrate was treated under lower tension (49 N m^{-1}), changes on a supramolecular level were more pronounced; in contrast, higher tension (147 N m^{-1}) had a limited affect on supramolecular changes. Moreover, treatment temperature has a greater effect on amorphous rather than crystalline regions.

Quantified values and comparison of bonded CBMs to amorphous regions of cellulose II-based polymers (as discriminated by CBM28) were compared with previously obtained Hydrogen Bond Intensity (HBI) data obtained from ATR-FTIR (Široký et al., 2010), shown in Fig. 5; in general HBI decreases with decrease in binding of CBM28 (increase in crystallinity). However, the reliability of the comparison varied under different treatment temperatures and tensions, and was not as reliable as the comparisons

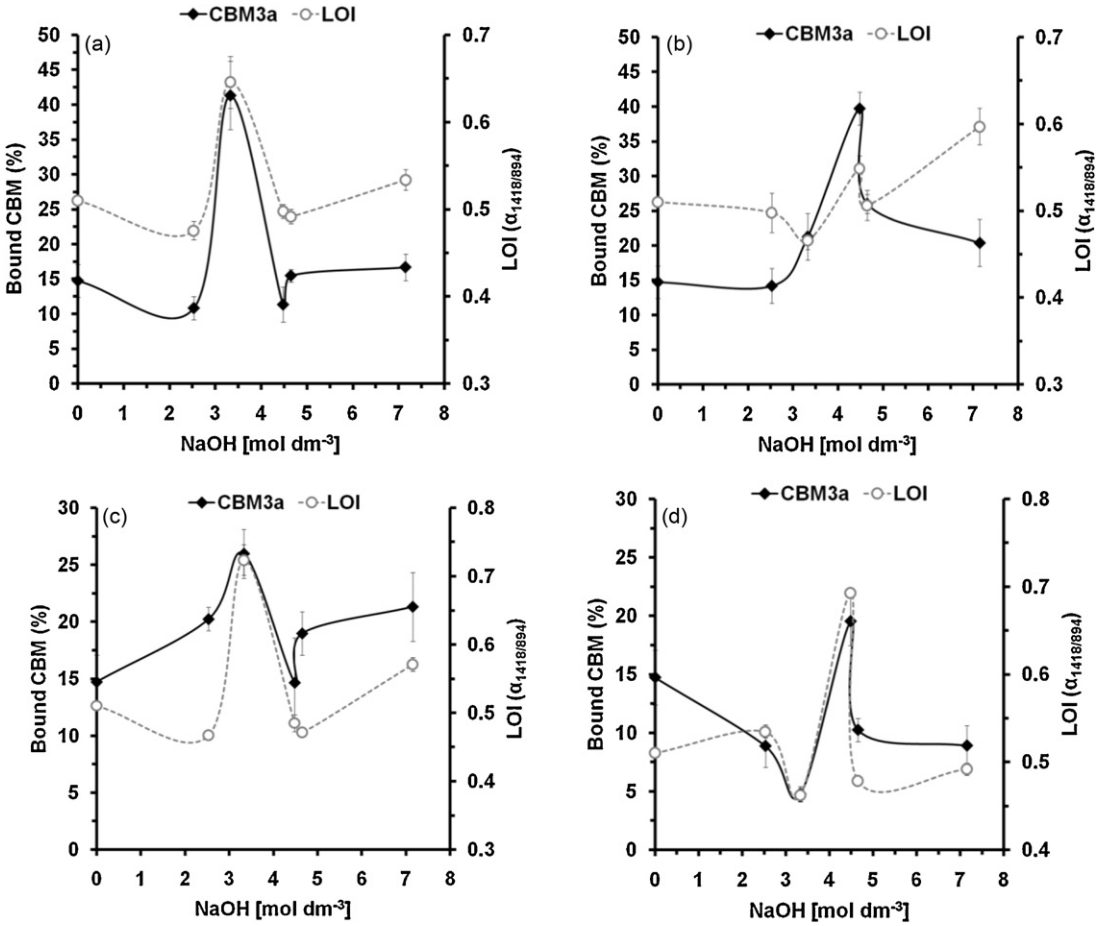

Fig. 4. Comparison of bonded CBM3a with LOI (Široký et al., 2010) with increasing NaOH concentration in treatment stage, under varying tension (49 or 147 N m^{-1}) and temperature (25 or 40 °C) in treatment stage of continuous alkali treatment: (a) 49/25; (b) 49/40; (c) 147/25; (d) 147/40.

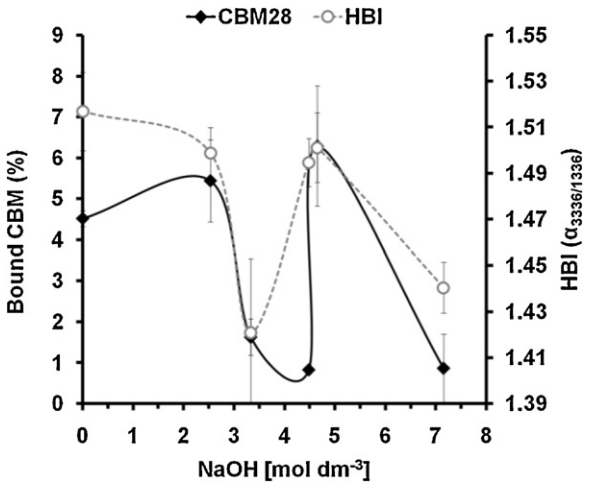

Fig. 5. Percentage of bonded CBM28 with HBI (Široký et al., 2010) increasing NaOH concentration in treatment stage, under tension of 147 N m^{-1} and temperature of 25 °C in treatment stage of continuous alkali treatment.

between CBM3a binding and TCI or LOI obtained from ATR-FTIR spectra.

It is clear that there is a wide range of possibilities or processes to influence the fiber structure and its properties during the manufacturing (regeneration) process. One of the processes mentioned herein is a "softer" precipitation, involving a two-stage precipitation in alcohol and water; by this process a decrease of crystallinity and orientation of lyocell fibers is obtained and, therefore, the core-shell structure of the fiber is affected (Klemm, Heublein, Fink, & Bohn, 2005). It is also known that the structure and properties of regenerated fibers, like density, crystallite size, orientation, pore number and volume, and therefore skin-core structure, can be influenced with applied physical process (spinning) conditions (Fink, Weigel, Purz, & Ganster, 2001; Krässig, 1993; Morehead & Sisson, 1945; Sisson, 1960; Tyler & Wooding, 1958). Recently, an important structure model describing the relationship between diffusion conditions and the resulting pore structure was proposed by Biganska (2002), wherein a skin-core model for lyocell fibers was proposed based on the morphology resulting from different precipitation conditions of blocks of *N*-methyl-*N*-morpholine-oxide-dissolved cellulose observed by microscopy. In it, three different parts are presented, a system with compact fiber core, a porous middle zone and a semi-permeable fiber skin; this was confirmed by Abu-Rous, Varga, Bechtold, and Schuster (2007) using a fluorescent dye molecular probe of lyocell fibers. However, Gindl, Martinschitz, Boesecke, and Keckes (2006) showed that only two different parts within lyocell fiber do exist, skin and core. The effect of fiber bending onto fiber orientation was studied on the tensile (higher orientation) and the compression (lower orientation) sides. Also, they observed that studied fibers have uniform skin-core orientation, in contrast, Kong et al. (2007) obtained non-uniform skin-core orientation by X-ray diffraction due to the

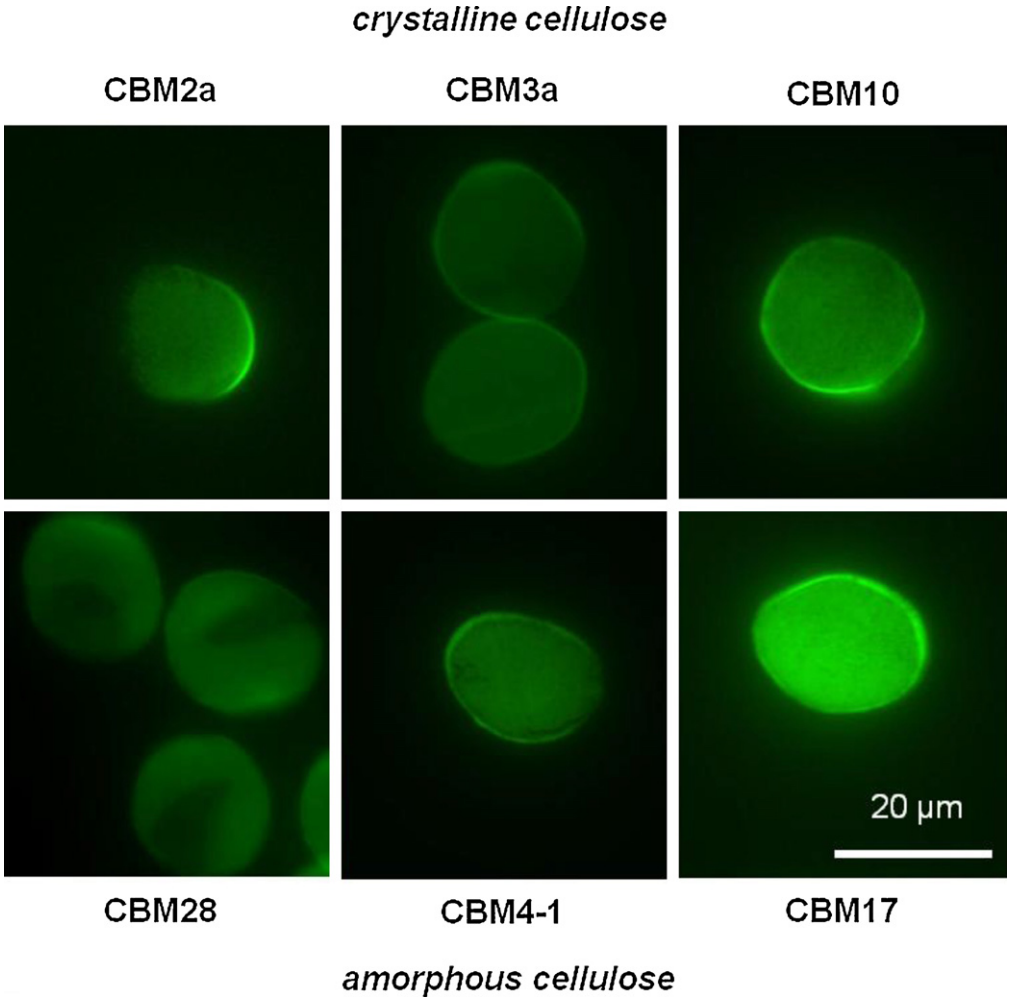

Fig. 6. Indirect immunofluorescence detection of CBMs binding to transverse-sections (thickness of 0.5 µm) of resin-embedded fibers.

differences of used beam size (5 μm × 5 μm *vs.* 500 nm). This non-uniformity resulted in the higher average orientation of the fiber skin than of the core. It was pointed out that the skin-core model of lyocell fibers is influenced by the increased shear forces on the outer region of the fiber during the passing the spinning dope through the spinneret, which generates higher crystal orientation at the skin.

From cross-sections of immunofluorescence labeled untreated lyocell (Fig. 6), it is revealed using different types of CBMs that the semi-permeable fiber skin does exist as both families of CBMs (both for crystalline and amorphous cellulose) bind strongly at the surface and demonstrate a very clear outer layer. It was discussed previously that this thin skin layer (about 100 nm) is comprised of only amorphous cellulose (Bredereck & Hermanutz, 2005). By employing immunofluorescence, only two regions were recognized and third one was not detected as proposed by Biganska (2002). Additionally, CBM17 binds extremely well to inert parts of fiber, core, it is known to have high affinity to amorphous cellulose of similar structure to CBM28 (Boraston, Ghaffari, Warren, & Kilburn, 2002; Boraston et al., 2003), which may have indicated a dominance of non-ordered regions within its structure. Herein, the suitability of this method to visualize/study the skin-core differences of fibers is demonstrated, which could be certainly a topic for further investigation.

4. Conclusions

The observations herein demonstrate that it is possible to use immunoassay labeling techniques as a versatile method offering the attractive capability to visualize the supramolecular changes of cellulose II-based substrates. By using an appropriate method, quantification of changes on a supramolecular level in cellulose is possible, which will contribute to a better understanding of macro- and microscopic fiber properties. Potentially it could yield more detailed information on where, for example, supramolecular changes in the fiber occurs, in comparison with bulk techniques (*e.g.* FT-IR, X-ray diffraction) that only measure the whole of the presented sample.

The changes in cellulose II-based polymer at supramolecular structure were visualized and successfully quantified. In terms of an increase in crystallinity, two maxima were observed, at concentrations of 3.33 and 4.48 mol dm^{-3} NaOH, under treatment conditions of 49 N m^{-1} at 25 °C, and 147 N m^{-1} at 40 °C, respectively. The observed changes and trends within amorphous regions may indicate a greater sensitivity to mechanical (applied tension), chemical (NaOH concentration), and thermal (treatment temperature) variations in the treatment process. By applying different types of CBMs, it was demonstrated that the semi-permeable fiber skin and a porous middle zone-core, do exist within lyocell fiber, and it is certainly an interesting topic for further detailed investigation.

Acknowledgements

The authors thank The University of Leeds and Lenzing AG for the provision of a scholarship to Mr. Široký. We thank Harry Gilbert for the provision of the CBMs and useful discussions.

References

Abu-Rous, M., Varga, K., Bechtold, T., & Schuster, K. C. (2007). A new method to visualize and characterize the pore structure of TENCEL (R) (Lyocell) and other man-made cellulosic fibres using a fluorescent dye molecular probe. *Journal of Applied Polymer Science*, *106*(3), 2083–2091.

Araki, Y., Karita, S., Tsuchiya, T., Kondo, M., & Goto, M. (2010). Family 17 and 28 carbohydrate-binding modules discriminated different cell-wall sites in sweet potato roots. *Bioscience, Biotechnology, and Biochemistry*, *74*(4), 802–805.

Barnette, A. L., Bradley, L. C., Veres, B. D., Schreiner, E. P., Park, Y. B., Park, J., et al. (2011). Selective detection of crystalline cellulose in plant cell walls with sum-frequency-generation (SFG) vibration spectroscopy. *Biomacromolecules*, *12*(7), 2434–2439.

Behera, B. K. (2004). Image-processing in textiles. *Textile Progress*, *35*(2–4), 1–193.

Bendayan, M., Nanci, A., & Kan, F. W. (1987). Effect of tissue processing on colloidal gold cytochemistry. *Journal of Histochemistry & Cytochemistry*, *35*(9), 983–996.

Biganska, O. (2002). *Etude physico-chemique des solutions de cellulose dans la N-methylmorpholine-Noxyde. Ecole des Mines de Paris (vol. PhD)*. Sophia Antipolis, France: Centre de Mise en Forme des Materiaux (CEMEF).

Blake, A. W., McCartney, L., Flint, J. E., Bolam, D. N., Boraston, A. B., Gilbert, H. J., et al. (2006). Understanding the biological rationale for the diversity of cellulose-directed carbohydrate-binding modules in prokaryotic enzymes. *Journal of Biological Chemistry*, *281*(39), 29321–29329.

Bolam, D. N., Ciruela, A., McQueen-Mason, S., Simpson, P., Williamson, M. P., Rixon, J. E., et al. (1998). Pseudomonas cellulose-binding domains mediate their effects by increasing enzyme substrate proximity. *Biochemical Journal*, *331*(3), 775–781.

Boraston, A. B., Chiu, P., Warren, R. A. J., & Kilburn, D. G. (2000). Specificity and affinity of substrate binding by a family 17 carbohydrate-binding module from Clostridium cellulovorans cellulase 5A. *Biochemistry*, *39*(36), 11129–11136.

Boraston, A. B., Ghaffari, M., Warren, R. A. J., & Kilburn, D. G. (2002). Identification and glucan-binding properties of a new carbohydrate-binding module family. *Biochemical Journal*, *361*, 35–40.

Boraston, A. B., Kwan, E., Chiu, P., Warren, R. A. J., & Kilburn, D. G. (2003). Recognition and hydrolysis of noncrystalline cellulose. *Journal of Biological Chemistry*, *278*(8), 6120–6127.

Boraston, A. B., Nurizzo, D., Notenboom, V., Ducros, V., Rose, D. R., Kilburn, D. G., et al. (2002). Differential oligosaccharide recognition by evolutionarily-related beta-1,4 and beta-1,3 glucan-binding modules. *Journal of Molecular Biology*, *319*(5), 1143–1156.

Bredereck, K., & Hermanutz, F. (2005). Man-made cellulosics. *Review of Progress in Coloration Nad other Topics*, *35*(1), 59–75.

Craig, S., & Miller, C. (1984). LR white resin and improved on-grid immunogold detection of vicilin, a pea seed storage protein. *Cell Biology International Reports*, *8*(10), 879–886.

Crawshaw, J., & Cameron, R. E. (2000). A small angle X-ray scattering study of pore structure in Tencel cellulose fibres and the effects of physical treatments. *Polymer*, *41*(12), 4691–4698.

Dagel, D. J., Liu, Y.-S., Zhong, L., Luo, Y., Himmel, M. E., Xu, Q., et al. (2011). In situ imaging of single carbohydrate-binding modules on cellulose microfibrils. *The Journal of Physical Chemistry B*, *115*(4), 635–641.

Fink, H. P., Weigel, P., Purz, H. J., & Ganster, J. (2001). Structure formation of regenerated cellulose materials from NMMO-solutions. *Progress in Polymer Science*, *26*(9), 1473–1524.

Gindl, W., Martinschitz, K. J., Boesecke, P., & Keckes, J. (2006). Orientation of cellulose crystallites in regenerated cellulose fibres under tensile and bending loads. *Cellulose*, *13*(6), 621–627.

Hashimoto, H. (2006). Recent structural studies of carbohydrate-binding modules. *Cellular and Molecular Life Sciences*, *63*(24), 2954–2967.

Heinze, U., & Wagenknecht, W. (1998). *Comprehensive cellulose chemistry. Functionalisation of cellulose*. Weinheim, Germany: Wiley-VCH.

Hess, M. W. (2003). Of plants and other pets: Practical aspects of freeze-substitution and resin embedding. *Journal of Microscopy*, *212*(1), 44–52.

Hogg, D., Pell, G., Dupree, P., Goubet, F., Martin-Orue, S. M., Armand, S., et al. (2003). The modular architecture of *Cellvibrio japonicus* mannanases in glycoside hydrolase families 5 and 26 points to differences in their role in mannan degradation. *Biochemical Journal*, *371*(3), 1027–1043.

Jamal, S., Nurizzo, D., Boraston, A. B., & Davies, G. J. (2004). X-ray crystal structure of a non-crystalline cellulose-specific carbohydrate-binding module: CBM28. *Journal of Molecular Biology*, *339*(2), 253–258.

Kawakubo, T., Karita, S., Araki, Y., Watanabe, S., Oyadomari, M., Takada, R., et al. (2010). Analysis of exposed cellulose surfaces in pretreated wood biomass using carbohydrate-binding module (CBM)-cyan fluorescent protein (CFP). *Biotechnology and Bioengineering*, *105*(3), 499–508.

Kellett, L. E., Poole, D. M., Ferreira, L. M. A., Durrant, A. J., Hazlewood, G. P., & Gilbert, H. J. (1990). Xylanase B and an arabinofuranosidase from *Pseudomonas fluorescens* subsp. cellulosa contain identical cellulose-binding domains and are encoded by adjacent genes. *Biochemical Journal*, *272*(2), 369–376.

Klemm, D., Heublein, B., Fink, H. P., & Bohn, A. (2005). Cellulose: Fascinating biopolymer and sustainable raw material. *Angewandte Chemie-International Edition*, *44*(22), 3358–3393.

Klemm, D., Philipp, B., Heinze, T., Heinze, U., & Wagenknecht, W. (1998). Fundamentals and analytical methods. *Comprehensive cellulose chemistry*. Weinheim, Germany: Wiley-VCH.

Kljun, A., Benians, T. A. S., Goubet, F., Meulewaeter, F., Knox, J. P., & Blackburn, R. S. (2011). Comparative analysis of crystallinity changes in cellulose I polymers using ATR-FTIR, X-ray diffraction, and carbohydrate-binding module probes. *Biomacromolecules*, *12*(11), 4121–4126.

Kolpak, F. J., & Blackwell, J. (1976). Determination of structure of cellulose II. *Macromolecules*, *9*(2), 273–278.

Kong, K., Davies, R. J., McDonald, M. A., Young, R. J., Wilding, M. A., Ibbett, R. N., et al. (2007). Influence of domain orientation on the mechanical properties of regenerated cellulose fibers. *Biomacromolecules*, *8*(2), 624–630.

Kono, H., & Numata, Y. (2004). Two-dimensional spin-exchange solid-state NMR study of the crystal structure of cellulose II. *Polymer*, *45*(13), 4541–4547.

Krässig, H. A. (1993). *Cellulose: Structure, accessibility and reactivity*. Yverdon, Switzerland: Gordon and Breach Science Publishers S.A.

Kroon-Batenburg, L. M. J., Bouma, B., & Kroon, J. (1996). Stability of cellulose structures studied by MD simulations. Could mercerized cellulose II be parallel? *Macromolecules*, *29*(17), 5695–5699.

Langan, P., Nishiyama, Y., & Chanzy, H. (1999). A revised structure and hydrogen-bonding system in cellulose II from a neutron fiber diffraction analysis. *Journal of the American Chemical Society*, *121*(43), 9940–9946.

Lehtio, J., Sugiyama, J., Gustavsson, M., Fransson, L., Linder, M., & Teeri, T. T. (2003). The binding specificity and affinity determinants of family 1 and family 3 cellulose binding modules. *Proceedings of the National Academy of Sciences of the United States of America*, *100*(2), 484–489.

Lonsdale, J. E., McDonald, K. L., & Jones, R. L. (1999). High pressure freezing and freeze substitution reveal new aspects of fine structure and maintain protein antigenicity in barley aleurone cells. *The Plant Journal*, *17*(2), 221–229.

McCartney, L., Blake, A. W., Flint, J., Bolam, D. N., Boraston, A. B., Gilbert, H. J., et al. (2006). Differential recognition of plant cell walls by microbial xylan-specific carbohydrate-binding modules. *Proceedings of the National Academy of Sciences of the United States of America*, *103*(12), 4765–4770.

McCartney, L., Gilbert, H. J., Bolam, D. N., Boraston, A. B., & Knox, J. P. (2004). Glycoside hydrolase carbohydrate-binding modules as molecular probes for the analysis of plant cell wall polymers. *Analytical Biochemistry*, *326*(1), 49–54.

McKie, V. A., Vincken, J. P., Voragen, A. G. J., van den Broek, L. A. M., Stimson, E., & Gilbert, H. J. (2001). A new family of rhamnogalacturonan lyases contains an enzyme that binds to cellulose. *Biochemical Journal*, *355*(1), 167–177.

McLean, B. W., Boraston, A. B., Brouwer, D., Sanaie, N., Fyfe, C. A., Warren, R. A. J., et al. (2002). Carbohydrate-binding modules recognize fine substructures of cellulose. *Journal of Biological Chemistry*, *277*(52), 50245–50254.

Morehead, F. F., & Sisson, W. A. (1945). Skin effect in viscose rayon. *Textile Research Journal*, *15*(12), 443–450.

Newman, G. R., & Hobot, J. A. (1987). Modern acrylics for post-embedding immunostaining techniques. *Journal of Histochemistry & Cytochemistry*, *35*(9), 971–981.

Okano, T., & Sarko, A. (1984). Mercerization of cellulose. 1. X-ray-diffraction evidence for intermediate structures. *Journal of Applied Polymer Science*, *29*(12), 4175–4182.

Park, S., Baker, J. O., Himmel, M. E., Parilla, P. A., & Johnson, D. K. (2010). Cellulose crystallinity index: Measurement techniques and their impact on interpreting cellulase performance. *Biotechnology for Biofuels*, 3.

Park, S., Johnson, D. K., Ishizawa, C. I., Parilla, P. A., & Davis, M. F. (2009). Measuring the crystallinity index of cellulose by solid state (13)C nuclear magnetic resonance. *Cellulose*, *16*(4), 641–647.

Raghothama, S., Simpson, P. J., Szabo, L., Nagy, T., Gilbert, H. J., & Williamson, M. P. (2000). Solution structure of the CBM10 cellulose binding module from Pseudomonas xylanase A. *Biochemistry*, *39*(5), 978–984.

Široká, B., Široký, J., & Bechtold, T. (2011). Application of ATR-FT-IR single-fiber analysis for the identification of a foreign polymer in textile matrix. *International Journal of Polymer Analysis and Characterization*, *16*(4), 259–268.

Široký, J., Blackburn, R. S., Bechtold, T., Taylor, J., & White, P. (2010). Attenuated total reflectance Fourier-transform Infrared spectroscopy analysis of crystallinity changes in lyocell following continuous treatment with sodium hydroxide. *Cellulose*, *17*(1), 103–115.

Široký, J., Blackburn, R. S., Bechtold, T., Taylor, J., & White, P. (2011). Alkali treatment of cellulose II fibres and effect on dye sorption. *Carbohydrate Polymers*, *84*(1), 299–307.

Široký, J., Manian, A. P., Široká, B., Abu-Rous, M., Schlangen, J., Bechtold, T., et al. (2008). Continuous alkali treatment process of plain woven lyocell fabrics: Effect of alkali concentration. In *Itc&Dc: 4th international textile clothing & design conference, book of proceedings* (pp. 453–458).

Široký, J., Manian, A. P., Široká, B., Abu-Rous, M., Schlangen, J., Blackburn, R. S., et al. (2009). Alkali treatments of Lyocell in continuous processes. I. Effects of temperature and alkali concentration on the treatments of plain woven fabrics. *Journal of Applied Polymer Science*, *113*(6), 3646–3655.

Sisson, W. A. (1960). The spinning of rayon as related to its structure and properties. *Textile Research Journal*, *30*(3), 153–170.

Thygesen, A., Oddershede, J., Lilholt, H., Thomsen, A. B., & Stahl, K. (2005). On the determination of crystallinity and cellulose content in plant fibres. *Cellulose*, *12*(6), 563–576.

Timms, B. G. (1986). Postembedding immunogold labeling for electron microscopy using LR White resin. *American Journal of Anatomy*, *175*(2–3), 267–275.

Tomme, P., Creagh, A. L., Kilburn, D. G., & Haynes, C. A. (1996). Interaction of polysaccharides with the N-terminal cellulose-binding domain of Cellulomonas fimi CenC. 1. Binding specificity and calorimetric analysis. *Biochemistry*, *35*(44), 13885–13894.

Tormo, J., Lamed, R., Chirino, A. J., Morag, E., Bayer, E. A., Shoham, Y., et al. (1996). Crystal structure of a bacterial family-III cellulose-binding domain: a general mechanism for attachment to cellulose. *Embo Journal*, *15*(21), 5739–5751.

Tyler, D. N., & Wooding, N. S. (1958). The determination and the significance of crystallite size in regenerated cellulose fibres. *Journal of the Society of Dyers and Colourists*, *74*(4), 283–291.

Warwicker, J. (1969). Swelling of cotton in alkalis and acids. *Journal of Applied Polymer Science*, *13*(1), 41–54.

Wells, B. (1985). Low temperature box and tissue handling device for embedding biological tissue for immunostaining in electron microscopy. *Micron and Microscopica Acta*, *16*(1), 49–53.

Xu, G. Y., Ong, E., Gilkes, N. R., Kilburn, D. G., Muhandiram, D. R., Harrisbrandts, M., et al. (1995). Solution structure of a cellulose-binding domain from cellulomonas fimi by nuclear magnetic resonance spectroscopy. *Biochemistry*, *34*(21), 6993–7009.